N84 27308

# SATELLITE REMOTE SENSING OVER ICE

Robert H. Thomas

California Institute of Technology
Jet Propulsion Laboratory
4800 Oak Grove Drive
Pasadena, CA 91109

Abstract: Satellite remote sensing provides unique opportunities for observing ice-covered terrain. Passive-microwave data give information on snow extent on land, sea-ice extent and type, and zones of summer melting on the polar ice sheets, with the potential for estimating snow-accumulation rates on these ice sheets. All weather, high-resolution imagery of sea ice is obtained using synthetic aperture radars, and ice-movement vectors can be deduced by comparing sequential images of the same region. Radar-altimetry data provide highly detailed information on ice-sheet topography, with the potential for deducing thickening/thinning rates from repeat surveys. The coastline of Antarctica can be mapped accurately using altimetry data, and the size and spatial distribution of icebergs can be monitored. Altimetry data also distinguish open ocean from pack ice and they give an indication of sea-ice characteristics.

## 1. INTRODUCTION

Most of the world's ice and snow lies in the polar regions, an area of some fifty million square kilometers that is sparsely populated and, to this day, poorly explored. Weather can be severe at any time of the year, clouds predominate over vast areas and, for several months each winter, there is no sunlight. Under these conditions, in situ scientific measurements are time-consuming and expensive, and they tend to be concentrated in locations of logistic convenience, with little or no coverage between these locations. Indeed, most of Antarctica remained unvisited and unmapped until after the Second World War, when extensive airborne surveys charted much of the coastline and most of the rock outcrops. More recently, a multi-year program of airborne radio-echo sounding of the ice cap has yielded maps of bedrock topography beneath approximately half of the ice sheet. However, spacing between flight lines was 50 to 100 km, and information density is sparse. Moreover, navigation is poor on most airborne surveys in polar regions and, unless well-defined control points exist within the survey area, there are significant errors in both positions and elevations of mapped features. Thus, mapping of the Antarctic ice sheet is still at a rudimentary level, with position errors of several kilometers and surface elevation errors of tens to hundreds of meters.

For many years, the study of polar ice was a pursuit for the dilettante eager to enjoy the scenery. More recently, however, our increased awareness of the role of polar ice in modulating and responding to polar climate, in controlling sea level, and in modifying ocean properties has exposed our lack of understanding of ice behavior. We do not know whether the ice sheets of Greenland and Antarctica are growing or shrinking; we do not know how much snow falls on these ice sheets,



PRECEDING PAGE BLANK NOT FILMED

how much surface melting there is, nor how much ice flows into the ocean to form icebergs; we cannot calculate accurately the forces that drive ice motion; and we cannot assess how strongly sea ice affects heat transfer between the ocean and atmosphere and hence influences both ocean properties and climate. We do know, however, that the polar regions are not dormant and unchanging. Wherever detailed measurements have been made, the ice sheet locally is either thickening or thinning, and there are major year-to-year changes in sea-ice cover that may influence weather conditions in areas far removed from the poles. We also know that predictions from climate models are strongly dependent on how sea ice is incorporated within the models. Indeed, sea-ice cover is often used as an adjustable parameter to force model predictions into verisimilitude at lower latitudes. For predictions of global-climate change due to factors such as increased $CO_2$, the climate models urgently need more realistic incorporation of sea-ice response.

Each of these problems can be addressed using data from satellite remote sensing. Indeed, these data provide our only source of synoptic observations over the polar regions. A major goal of the NASA research program in the polar regions is to improve our ability to convert satellite measurements into useful geophysical parameters. In this paper, I shall briefly review satellite remote-sensing techniques for observing ice cover, provide examples of derived products, and describe some of my own work on applications of altimetry data over ice.

## 2. REMOTE-SENSING TECHNIQUES

Until the advent of satellite observations, little was known about seasonal and year-to-year changes in sea-ice cover. Weather satellites of the National Oceanic and Atmospheric Administration (NOAA) still provide daily images of the polar regions with a spatial resolution of 1 to 4 km, and these are routinely used by the Navy/NOAA Joint Ice Center to provide weekly analyses of global sea-ice cover. Higher resolution imagery (tens of meters) is obtained by Landsat, but not on a regular basis; special arrangements must be made to obtain images over specific areas. Moreover, all visible and infrared imagery is severely limited by darkness and/or clouds. In order to overcome this problem, NASA has developed sensors to obtain microwave data, which provide information day and night in all weathers. Here, I shall focus attention on these microwave techniques.

### Microwave radiometers

All matter radiates electromagnetic energy as a consequence of molecular interaction. The energy is emitted over a range of wavelengths, the precise mix being determined by viewing angle, molecular composition, temperature, and material structure. Ice and liquid water have very distinct emission signatures, primarily because of differences in the way molecules are arranged in each. Moreover, different ice samples can have distinct signatures, partly because of temperature differences and partly because of differences in texture and impurity content. Snow density, grain size, surface roughness, brine content, and the degree of wetness all influence the radiated energy, and they influence it differently at different wavelengths. Thus, by sampling an appropriate suite of wavelengths the ice cover can be distinguished from open water and classified according to its surface and near-surface characteristics.

ORIGINAL PAGE IS
OF POOR QUALITY

For snow and ice on land, passive-microwave data potentially distinguish extent, water equivalent and onset of snow melt for seasonal snow cover (Kunzi et al., 1982) and the regions where summer melting occurs on the terrestrial ice sheets of Greenland and Antarctica (Zwally and Gloersen, 1977). Some of these applications are still research topics but they promise to become operational tools within the near future. In addition, it may be possible to deduce snow-accumulation rates over the polar ice sheets (Zwally, 1977; Rotman et al., 1982). Over sea ice, passive-microwave data can distinguish water from ice and characterize the major ice types: new ice, just a few cm thick; first-year ice, generally snow covered and up to 2 m thick; and old ice, which has survived at least one summer, has undergone deformation and cracking, and is of variable thickness with a comparatively hummocky surface. Old ice is also distinctive in having lower salinity than younger ice, and this gives it a distinctive microwave signature. In this paper, I shall refer to this old ice as "multiyear ice." In principle, the relative concentrations of water and each of the major ice types can be distinguished using passive-microwave data at appropriate wavelengths. Major problems occur, however, during the summer season when the existence of liquid water on the ice surface significantly affects the microwave emissions. This problem is currently under invescigation by several NASA-funded researchers (Comiso, 1983 ; Comiso et al., 1984; Carsey, In press).

The spatial resolution of a microwave sensor increases as the wavelength decreases or as the antenna size increases. Thus, high resolution can readily be obtained in the visible and infrared, but these short-wavelength radiations are strongly affected by atmospheric conditions, particularly clouds. Microwave radiations lie in the frequency range of 1 - 300 GHz (wavelengths from about 1 mm to 37 cm). They penetrate clouds and can provide all-weather, day/night synoptic

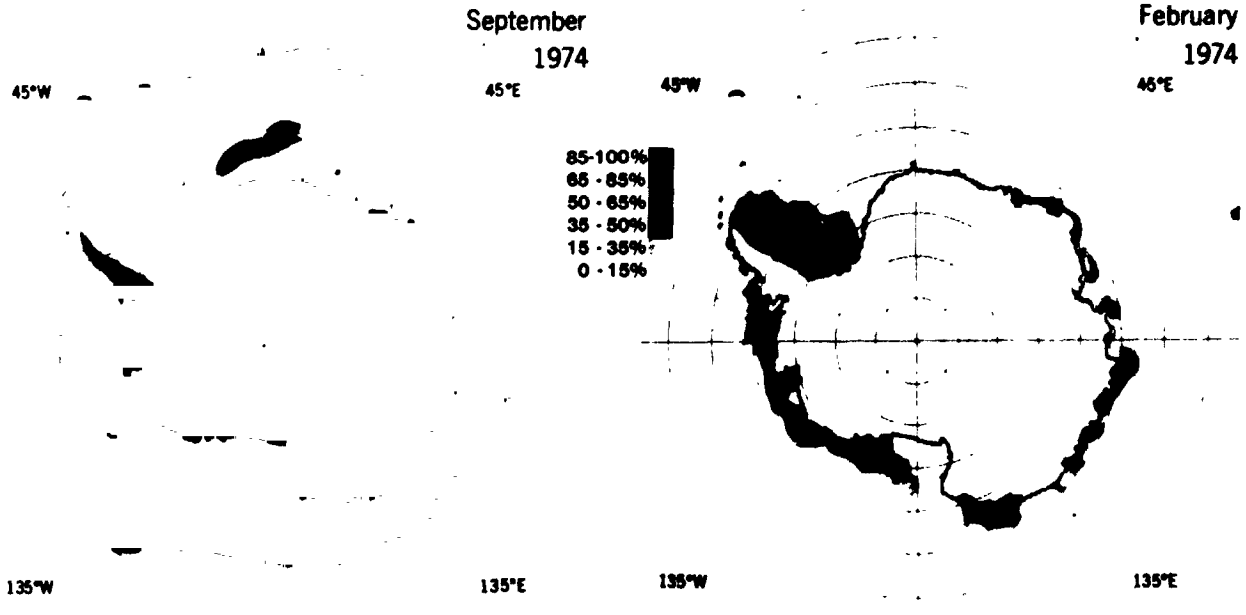


Figure 1. The contrast between winter maximum and summer minimum Antarctic sea-ice cover is clearly shown by these images obtained using ESMR data, with ice concentration depicted by different grey shades. From Zwally et al., 1983a.

ORIGINAL PAGE IS
OF POOR QUALITY

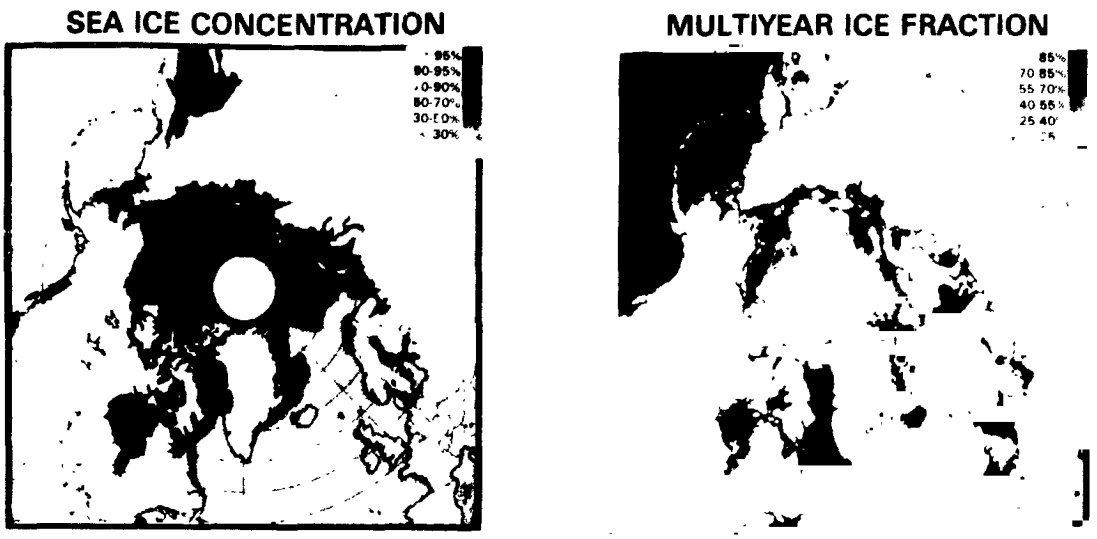


Figure 2. Arctic sea-ice concentrations and multiyear ice fractions for February 3-7, 1979, derived from SMMR data. From Cavalieri et al., In press, and included here by kind permission of D. Cavalieri.

measurements of several Earth-surface and atmospheric parameters (Njoku, 1982). The first satellite sensor to provide global information on ice extent was the Electrically Scanning Microwave Radiometer (ESMR), launched by NASA aboard Nimbus-5 in December 1972. It measured horizontally polarized radiation at 19.35 GHz with a spatial resolution of about 30 km, and useful swath width of 1400 km. Because measurements were made at only one frequency, there is ambiguity in data interpretation. However, estimates of ice concentration can be made to an accuracy of about $\pm$ 15% in areas where the ice cover is more or less homogeneous. Antarctic sea ice fulfills these requirements, and ESMR data have been analyzed to give a time series of Antarctic sea-ice cover from 1973 through 1976 (Zwally et al., 1983a). Figure 1 shows the contrast between summer minimum and winter maximum ice cover for 1974. The open water "polynya" straddling the Greenwich meridian in the winter image was first detected in ESMR data. It does not form every winter, and why it forms is not fully understood. It may be initiated by wind action, but its survival through the winter must require major upwelling of warm ocean water.

The quality of ESMR data deterioriated after 1976, but they were still used for operational ice forecasting by the Navy/NOAA Joint Ice Center until 1983. In October, 1978, the Scanning Multichannel Microwave Radiometer (SMMR) was launched aboard Nimbus-7. It has provided excellent data since then and is expected to continue operating into the mid 80's. SMMR acquires data in both vertical and horizontal polarization at these five frequencies: 6.6, 10.7, 18, 21, and 37 GHz. Spatial resolution ranges from 30 to 150 km, depending on frequency, and swath width is 780 km. Data from the 18 and 37 GHz channels are used to obtain estimates of both total sea-ice concentration and how much multiyear ice there is (Cavalieri et al., in press). Figure 2 shows estimates of total ice concentration and multiyear fraction for Feb. 3-7, 1979.

ORIGINAL PAGE IS
OF POOR QUALITY

Starting in 1985, a series of U.S. Defense Meteorological Satellite Program (DMSP) spacecraft will carry the Special Sensor Microwave/Imager (SSM/I), a scanning microwave radiometer that will collect data from a 1300 km swath in both vertical and horizontal polarization at 19.35, 37 and 85.5 GHz, and at 22.235 GHz in vertical polarization only. Spatial resolution will be between 12 and 50 km, depending on frequency. Sea-ice parameters will be obtained from the 19.35 and 37 GHz data and, potentially, from the 85.5 GHz data, which will provide better spatial resolution and may improve discrimination of ice types. NOAA plans to archive all SSM/I data, and NASA will process the data to higher-level products for research purposes.

Passive-microwave data provide excellent global synoptic coverage at low spatial resolution. Over the next decade, large-antenna radiometers will be developed, and resolution will improve to perhaps the 1 km level. Inevitably, data rates will increase and they will require improved techniques for processing and distribution.

Synthetic Aperature Radar (SAR)

The spatial resolution that can be achieved by a conventional radar is determined by radar frequency and antenna size. This imposes a practical limitation on the resolution. The SAR overcomes this by illuminating a swath off to the side of the spacecraft and discriminating individual resolution cells within the field of view according to range and Doppler shift in frequency due to spacecraft motion. The L-band SAR aboard NASA's Seasat, which operated from July to October, 1978, had a spatial resolution of 25 m and swath width of 100 km. Data were obtained at too high a rate (c. 100M bits per second) to be stored aboard the satellite, and they were transmitted in real time to appropriate receiving stations. A

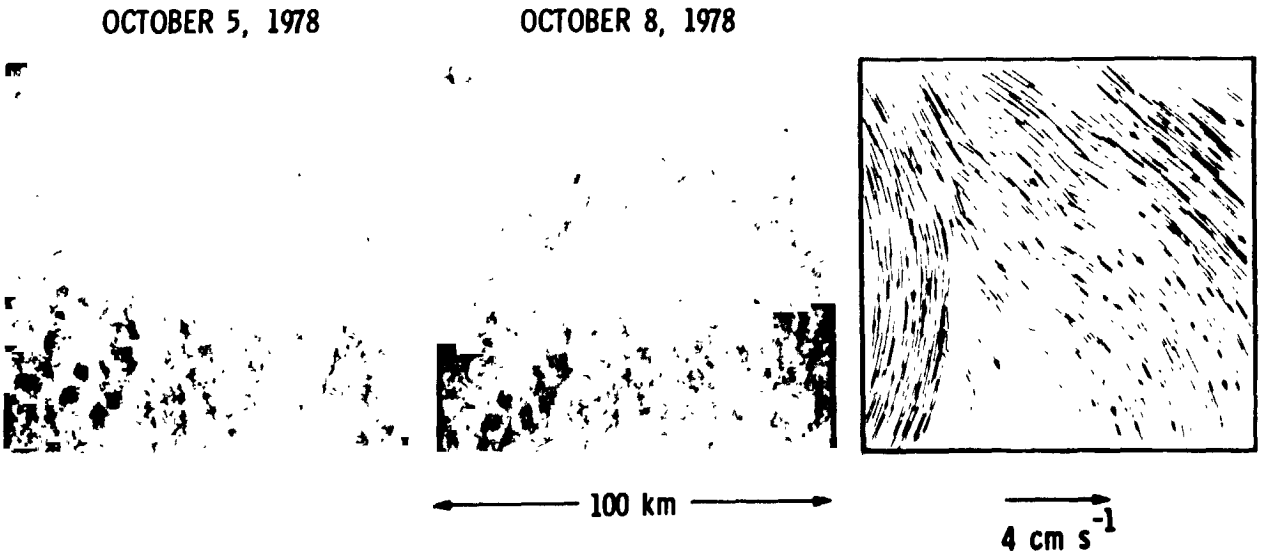


Figure 3. Seasat SAR images of Arctic pack ice taken 3 days apart, and velocity vectors obtained by comparing the positions of common floes in the two images. From Rothrock and Thorndike, In press, and included here by kind permission of D. Rothrock.

complex processing sequence yields a digital image of the illuminated swath with intensity proportional to radar backscatter, and an absolute position accuracy of about 100 m (Fu and Holt, 1982; Carsey et al., 1983).

Seasat clearly demonstrated the capability of using satellite SAR data to obtain all-weather, high-resolution imagery over sea ice. Figure 3 shows two SAR images of pack ice in the Beaufort Sea taken 3 days apart, with velocity vectors obtained by comparing positions of individual ice floes (Rothrock and Thorndike, In press). The images are filled with ice floes separated by dark areas of either open-water leads or very new ice. Many of the floes appear to be a patchwork of smaller units separated by light-shaded streaks, which may represent collision lines where ice has piled up to form ridges rising several meters above sea level. Current NASA research is focussed on developing automated techniques for analysing SAR sea-ice imagery to give ice-motion vectors and to characterize the ice by type.

Upcoming Space Shuttle missions will provide opportunities to acquire SAR data over sea ice for short periods and to test data-analysis techniques at different SAR frequencies. The next satellite SAR will operate at C-band aboard the European Space Agency's Remote Sensing Satellite (ERS-1), due to be launched in 1987/88. This should provide excellent sea-ice information, and NASA plans to establish a ground receiving station in Alaska to acquire ERS-1 SAR data over the Bering, Chukchi and Beaufort seas. There will also be ESA and Canadian receiving stations in Kiruna, Sweden and Prince Albert, Canada and, together with the NASA station, they will be capable of collecting data from most of the area covered by Arctic sea ice. Another satellite with the acronym ERS-1 will be launched by Japan in 1990, and this also will carry a SAR. Future prospects include acquisition of data over Antarctica, where the ice-sheet coastline could be mapped to an accuracy of about 100 m using SAR data.

Altimetry

Radar altimeters were carried aboard NASA's Geos-3 (April, 1975 to December, 1978) and Seasat (July to October, 1978). The Geos-3 orbit lay between latitudes 65°N and 65°S, and the data were used to improve significantly the surface-elevation map of the Greenland ice sheet (Brooks et al., 1978). Seasat extended coverage to 72° latitude and provided considerably greater accuracy. These altimeters were designed to measure ranges to the ocean surface by transmitting short radar pulses and measuring the time delay until receipt of the reflected pulse. Pulse rate was approximately 1000 per second and the altimeter was designed to track the half-power point on the leading edge of a composite return pulse formed by summing 50 consecutive received pulses. Summation took account of range changes between pulses by correcting delay times for range rate calculated from earlier measurements. In order to obtain high range resolution, return energy was measured only within a data-acquisition window of about 190 ns duration - equivalent to a range window 15 m above and below the measured surface.

The altimeters worked well over the oceans, where measured ranges change very slowly. But over sloping or undulating terrain, the servo-tracking circuit was not sufficiently agile to monitor rapidly changing ranges, and the altimeter frequently lost track of the return pulse. Although this resulted in short periods (usually a few seconds) when no useful data were obtained, the Seasat

ORIGINAL PAGE IS
OF POOR QUALITY

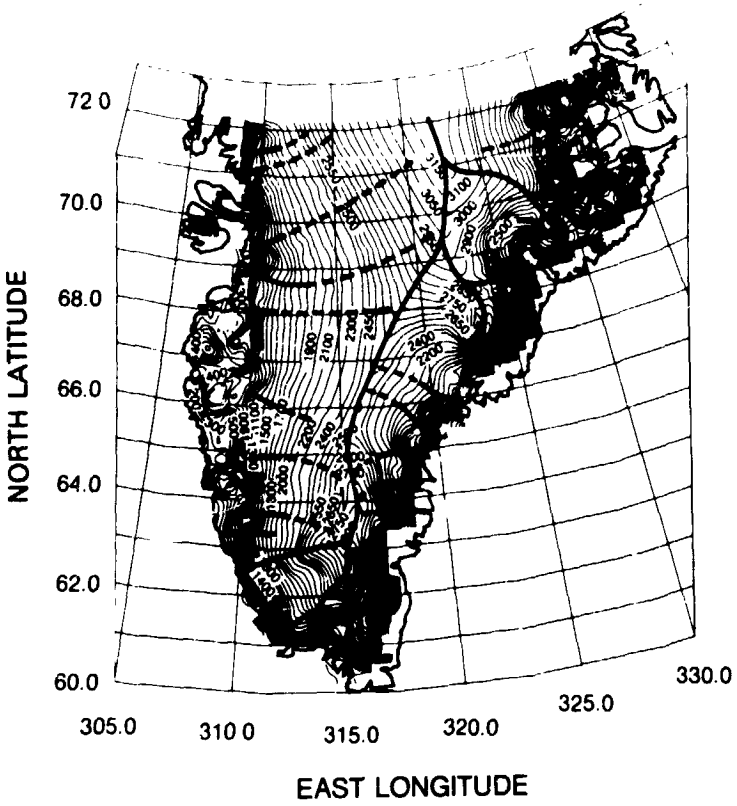


Figure 4. Ice surface topography over Greenland, derived from Seasat altimetry data. The heavy lines delineate drainage basins. From Bindschadler, In Press, and included here by kind permission of R. Bindschadler.

altimeter measured more than 600,000 useful elevations on the ice sheets of Greenland and Antarctica (Zwally et al., 1983b). It is important to note, however, the physical significance of these measured elevations. The radar beam produced a beam-limited footprint (BLF) of about 12 km radius, in contrast to the pulse-limited footprint (PLF) from which reflections comprising the leading edge of the return pulse were obtained. Over the ocean, the PLF had a radius between 1 and 5 km, depending on wave height, and measured ranges gave the average sea-surface elevation within the footprint. Over an ice sheet, however, spacing between surface undulations approaches the BLF radius, and the altimeter preferentially measured ranges to the closest undulation summits, averaging the effects of small-scale roughness, such as sastrugi. These summits were not necessarily directly beneath the satellite, leading to ambiguity when measured ranges are translated into surface elevations. Nevertheless, satellite radar altimeters provide the best available data for mapping ice-sheet topography over the vast areas of Greenland and Antarctica. The resulting surface represents a smoothed envelope biased slightly above the actual surface (Fig. 4). The smoothing distance is on the order of a few km, and the bias depends on local regional slope, undulation amplitude, and altimeter characteristics. To some extent, bias errors due to the regional slope can be corrected (Brenner et al., 1983).

ORIGINAL PAGE IS
OF POOR QUALITY

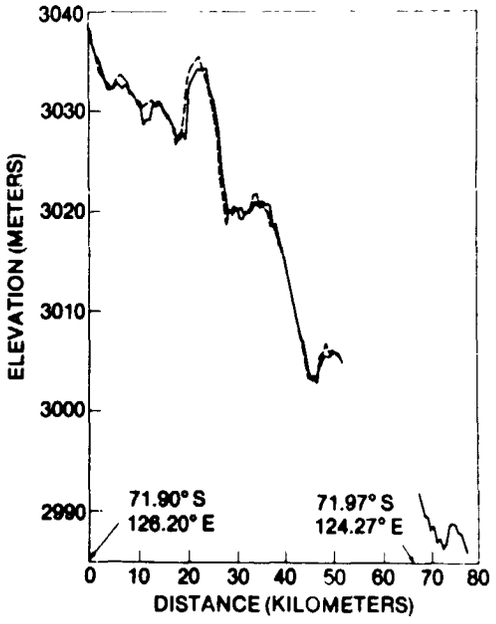


Figure 5. Two Seasat-altimetry profiles over the Antarctic ice sheet separated by about 40 m. From Zwally et al., 1983b.

The smoothed envelope obtained in this way is well suited to most glaciological requirements. Moreover, intercomparison of surfaces obtained from two altimetry missions a decade or so apart would provide clear indication of any regional changes in ice topography, since the local biasses would be approximately the same for each survey. Here, however, it is important to note that altimeter design characteristics must be similar for both surveys. Figure 5 shows two sets of Seasat measurements along repeat tracks over Antarctica, and gives an indication of how well the altimeter performed over ice. Range accuracy over smoother portions of the ice sheet was $\pm$ 25 cm.

Return pulses over oceans and ice sheets generally have a similar shape, with a fairly sharp rise and a slow decay. But over sea ice, the return pulse has a much sharper rise followed by a quite rapid fall producing a spike characteristic of a specular reflection. In principle, the shape of this spike can give information on sea-ice characteristics, such as surface roughness, amount of open water within the footprint, and ocean swell within the pack ice. However, caution must be exercised in analysing existing altimetry data since significant range-rate errors over sea ice lead to appreciable broadening of the pulse shape in the Seasat data record, which was formed by summing two adjacent 50-pulse composites. Nevertheless, the altimetry data provide an accurate indication of the boundary between open ocean and sea ice.

Future altimetry missions will be flown aboard the U.S. Navy's Geosat (to be launched in 1984), ESA's ERS-1 (1987/8) and the U.S. Navy/NASA/NOAA joint mission NROSS (1989). Anticipated changes in altimeter design will probably yield significant improvements in performance over ice. Moreover, although Geosat will repeat approximately the Seasat coverage, ERS-1 and NROSS will provide data to 82° latitude.

ORIGINAL PAGE IS
OF POOR QUALITY

## 3. MAPPING COASTAL ICE CLIFFS AND ICEBERGS FROM ALTIMETRY DATA

In a recent paper Thomas et al., (1983) showed how the coast of Antarctica could be mapped using satellite altimetry data. As it approached the continent from the ocean, the Seasat altimeter obtained strong reflections from sea ice even for a short time after passing over the ice front (Fig. 6). Measured ranges were oblique distances to the nearest portion of sea ice, yielding an apparent drop in surface elevation. The sequence of oblique ranges gives the position of the sea ice along a segment of the ice cliff that forms much of the Antarctic coastline. The entire Seasat data set provides an opportunity for mapping this coastline to an accuracy of $\pm$ (0.1 to 1 km), representing a major improvement over existing surveys. Moreover, as the altimeter approached the ice cliff, the intensity of the radar signal arriving prior to the sea-ice reflection increased due to reflections from the ice surface inland from the ice cliff. This pre-pulse intensity reaches a maximum near the point where the satellite crossed over the ice cliff, and then diminishes. At the same time, the intensity of the sea-ice reflection decreases as the reflection becomes more oblique. This is well

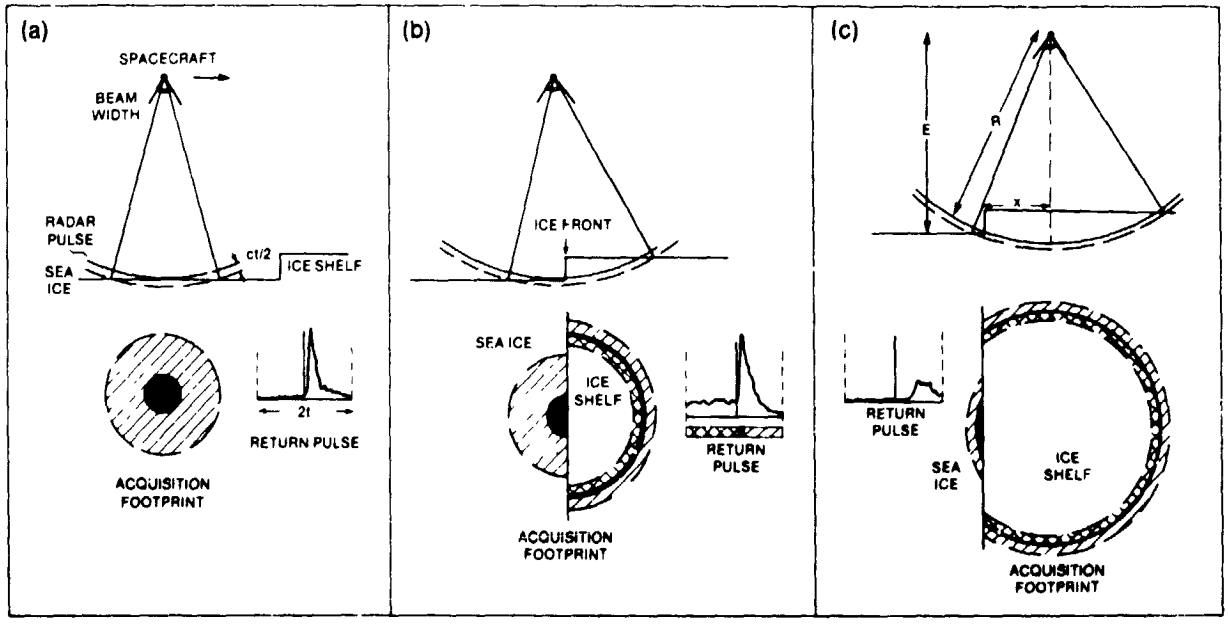


Figure 6. Radar altimeter approaching an ice shelf and continuing to measure ranges to nearby sea ice after crossing the ice front. The radar pulse is of very short duration and is represented by the solid line. The acquisition footprint (cross-hatched area in (a)) indicates the area from which reflections can be received during the data-acquisition window (of duration 2t). The pulse-limited footprint (about 1 km radius) is the black area; the area from which reflections are received prior to the main return is double cross-hatched; the area contributing to the trailing edge of the return pulse is single cross-hatched. c is the velocity of light. From Thomas et al., 1983.

ORIGINAL PAGE IS
OF POOR QUALITY

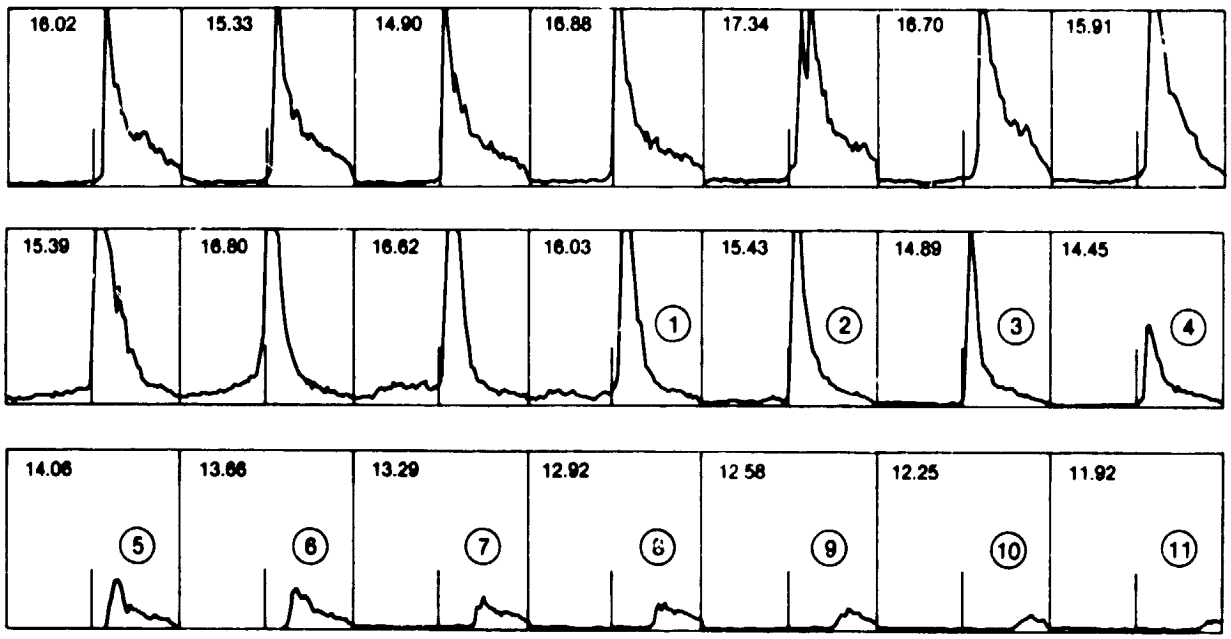


Figure 7. Reflected radar pulses obtained at intervals of 0.1 s by the Seasat altimeter as it approached from seaward, and then crossed Amery Ice Front. Each frame represents a time window of duration of about 188 ns, equivalent to an elevation difference of about 28 m. The numbers in each frame give the altimeter-derived surface elevation in meters above the ellipsoid. This elevation, before correction for lags in the tracking circuit, corresponds to the time of the short vertical line in the center of the window. Frames (1) to (11) represent oblique ranges to sea with the satellite over the ice shelf. From Thomas et al., 1983.

illustrated in Figure 7, where a sequence of reflected pulses are shown for a Seasat orbit approaching, and then passing over, the Amery Ice Shelf in Antarctica. Figure 8 shows the apparent surface elevation of the sea ice and the pre-pulse intensity plotted against distance along the subsatellite track.

Similar effects are noticed when the altimeter passed over icebergs. On each side of the iceberg there was a rise in pre-pulse intensity; over the iceberg, both the intensity of the sea-ice return and the measured surface elevation decreased. Figure 9 shows this sequence, obtained when Seasat passed over an iceberg near the Greenwich meridian off the coast of Antarctica. The Seasat data set contains many such examples, which we are currently analysing to obtain an estimate of iceberg sizes and distribution. Moreover, even icebergs that were not directly beneath the satellite left an imprint in the data record, since they elevated the pre-pulse intensity so long as they lay within the BLF. This provides a powerful technique for monitoring iceberg population in Antarctic waters, and indirectly obtaining an estimate of ice discharge from the continent.

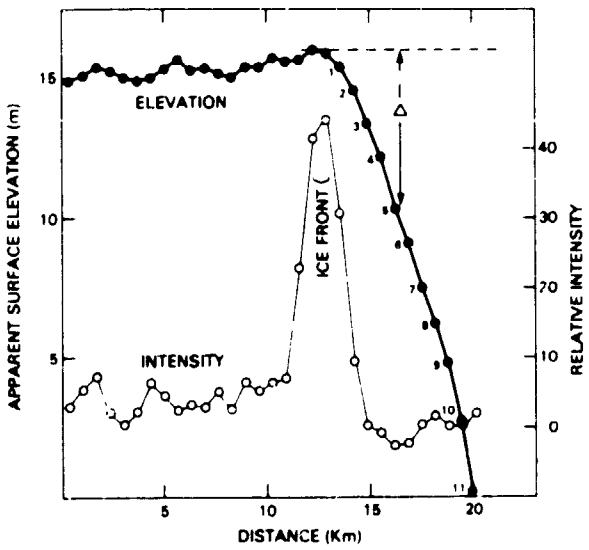


Figure 8. Apparent surface elevation versus distance along the subsatellite track for an orbit crossing Amery Ice Front. Also shown is the average intensity, in arbitrary units, of the pre-pulse radar reflection. From Thomas et al., 1983.

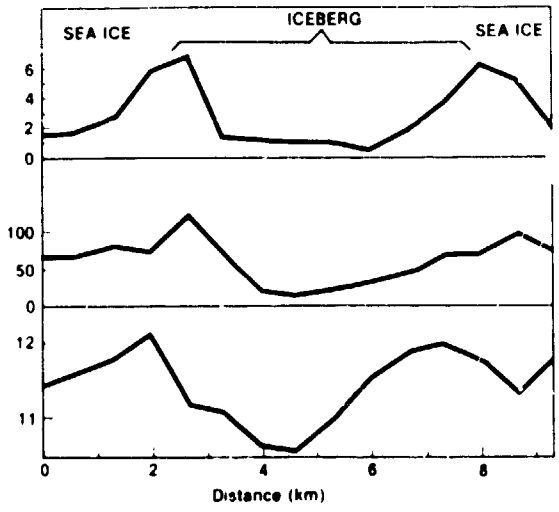


Figure 9. Measurements deduced from altimetry data obtained on 28 July, 1978, as Seasat passed over an iceberg surrounded by sea ice at 69.8°S, 2.4°W. The top plot shows pre-pulse intensity; the middle plot shows peak intensity of the main return; the lower plot shows apparent surface elevation derived from the altimetry data. Ordinates on the top and middle plots are arbitrary units, on the lower plot they are meters above the Earth ellipsoid. Abscissa is distance in km along the subsatellite track.

Acknowledgements: Most of the work reviewed here is being conducted by investigators funded by NASA'S Oceanic Processes Branch, and I have benefitted particularly from numerous discussions with D. Cavalieri, J. Comiso and J. Zwally at Goddard Space Flight Center, F. Carsey at the Jet Propulsion Laboratory and D. Rothrock at the University of Washington.

## REFERENCES

Bindschadler, R. A., In press: Jacobshavn Glacier drainage basin: a balance assessment. J. Geophys. Res.

Brenner, A. C., R. A. Bindschadler, R. H. Thomas, and H. J. Zwally, 1983: Slope-induced errors in radar altimetry over continental ice sheets. J. Geophys. Res., 88, 1617-1623.

Brooks, R. L., W. J. Campbell, R. O. Ramseier, H. R. Stanley, and H. J. Zwally, 1978: Ice sheet topography by satellite altimetry. Nature, 274, 539-543.

Cars F. D., In press: Summer Arctic sea ice character from satellite microwave data. J. Geophys. Res.

Carsey, F. D., J. Curlander, B. Holt, and K. Hussey, 1983: Shear zone ice deformation using supervised analysis of Seasat data. AIAA 21st Aerospace Sciences Meeting, Reno, Nevada.

Cavalieri, D. J., P. Gloersen, and W. J. Campbell. In press: Determination of sea ice parameters with the Nimbus-7 SMMR. J. Geophys. Res.

Comiso, J. C., 1983: Sea ice effective microwave emissivities from satellite passive microwave and infrared observations. J. Geophys. Res., 88, 7686-7704.

Comiso, J. C., S. F. Ackley, and A. L. Gordon, 1984: Antarctic sea ice microwave signatures and their correlation with in situ ice observations. J. Geophys. Res., 89, 662-672.

Fu, L.-L. and B. Holt, 1982: Seasat views oceans and sea ice with synthetic-aperture radar. JPL Publication 81-120. Jet Propulsion Laboratory, Pasadena, California, 200p.

Kunzi, K. F., S. Patil, and H. Rott, 1982: Snow-cover parameters retrieved from Nimbus-7 Scanning Multichannel Microwave Radiometer (SMMR) data. IEEE Trans. Geosci. Remote Sensing, GE-20, 452-467.

Njoku, E. G., 1982: Passive microwave remote sensing of the Earth from space - a review. Proc. IEEE., 70, 728-750.

Rothrock, D. A. and A. S. Thorndike, In press: Measuring sea-ice floe size distribution. J. Geophys. Res.

Rotman, S. R., A. D. Fisher, and D. H. Staelin, 1982: Inversion for physical characteristics of snow using passive radiometric observations. J. Glaciol., 28, 179-185.

Thomas, R. H., T. V. Martin, and H. J. Zwally, 1983: Mapping ice-sheet margins from radar altimetry data. Annals of Glaciology, 4, 283-288.

Zwally, H. J., 1977: Microwave emissivity and accumulation rate of polar firn. J. Glaciol., 18, 195-215.

Zwally, H. J. and P. Gloersen, 1977: Passive microwave images of the polar regions and research applications. Polar Record, 18, 431-450.

Zwally, H. J., J. C. Comiso, C. L. Parkinson, W. J. Campbell, F. D. Carsey, and P. Gloersen, 1983a: Antarctic sea ice, 1973-1976: satellite passive-microwave observations. NASA SP-459, NASA, Washington, D.C., 206p.

Zwally, H. J., R. A. Bindschadler, A. C. Brenner, T. V. Martin, and R. H. Thomas, 1983b: Surface elevation contours of Greenland and Antarctic ice sheets. J. Geophys. Res., 88, 1589-1596.